Polarization-induced transport in ferroelectric organic field-effect transistors

ARTICLE *in* JOURNAL OF APPLIED PHYSICS · MARCH 2015

Impact Factor: 2.18 · DOI: 10.1063/1.4914415

2 AUTHORS:

Amrit Laudari
University of Missouri
5 PUBLICATIONS **4** CITATIONS
SEE PROFILE

Suchismita Guha
University of Missouri
120 PUBLICATIONS **1,181** CITATIONS
SEE PROFILE

AIP | Journal of Applied Physics

Polarization-induced transport in ferroelectric organic field-effect transistors

A. Laudari and S. Guha

Citation: Journal of Applied Physics **117**, 105501 (2015); doi: 10.1063/1.4914415
View online: http://dx.doi.org/10.1063/1.4914415
View Table of Contents: http://scitation.aip.org/content/aip/journal/jap/117/10?ver=pdfcov
Published by the AIP Publishing

JOURNAL OF APPLIED PHYSICS **117**, 105501 (2015)

Polarization-induced transport in ferroelectric organic field-effect transistors

A. Laudari and S. Guha[a)]
Department of Physics and Astronomy, University of Missouri, Columbia, Missouri 65211, USA

(Received 3 February 2015; accepted 27 February 2015; published online 10 March 2015)

Ferroelectric dielectrics, permitting access to nearly an order of magnitude range of dielectric constants with temperature as the tuning parameter, offer a great platform to monitor the changes in interfacial transport in organic field-effect transistors (OFETs) as the polarization strength is tuned. Temperature-dependent transport studies have been carried out from pentacene-based OFETs using the ferroelectric copolymer poly(vinylidene fluoride-co-trifluoroethylene) (PVDF-TrFE) as a gate insulating layer. The thickness of the gate dielectric was varied from 20 nm to 500 nm. By fits to an Arrhenius-type dependence of the charge carrier mobility as a function of temperature, the activation energy in the ferroelectric phase is found to increase as the thickness of the PVDF-TrFE layer decreases. The weak temperature-dependence of the charge carrier mobility in the ferroelectric phase of PVDF-TrFE may be attributed to a polarization fluctuation driven transport, which results from a coupling of the charge carriers to the surface phonons of the dielectric. By comparing single layer PVDF-TrFE pentacene OFETs with stacked PVDF-TrFE/inorganic dielectric OFETs, the contribution from Fröhlich polarons is extracted. The temperature-dependent mobility of the polarons increases with the thickness of the PVDF-TrFE layer. Using a strongly coupled polaron model, the hopping lengths were determined to vary between 2 Å and 5 Å. © *2015 AIP Publishing LLC*. [http://dx.doi.org/10.1063/1.4914415]

I. INTRODUCTION

Since the discovery of the piezoelectric effect in ferroelectric polymers such as poly(vinylidene fluoride) (PVDF) more than 40 years,[1] considerable efforts have been made in using PVDF and its copolymers with trifluoroethylene (TrFE) as the gate dielectric layer in organic field-effect transistors (OFETs) including graphene field-effect transistors, for memory and other applications.[2–7] Understanding the role of the dielectric layer in interfacial charge transport processes has been equally important. The general mechanism of transport in these devices takes place in the framework of localized states giving rise to hopping transport and polaronic models.[8,9] The polaronic nature of the charge carriers is heavily masked by disorder effects.[10] Theory reveals the importance of both local and non-local electron-phonon coupling for a comprehensive understanding of the charge transport mechanism.[11] The dynamic coupling of charge carriers to the electronic polarization at the semiconductor-dielectric interface mainly arises from two effects: the image force due to the polarization discontinuity at the interface and the Coulomb interaction of the charge carriers with the surface phonons of the dielectric,[12,13] schematically shown in Fig. 1. It has been shown that Fröhlich surface polarons are formed if the gate dielectric is sufficiently polar in molecular systems.[14] A dynamic coupling of the Fröhlich polarons is also observed in ionic liquid gate dielectrics.[15] The Fröhlich polarons reflect a long-range interaction between the charge carriers and the longitudinal optical (LO) phonons. It is these interactions at the interface that result in a renormalization of the transfer integral for the transport process and manifests itself as reduced charge carrier mobility when the dielectric constant of the gate insulator increases.

Several models have been proposed to describe charge transport in organic materials: variable range hopping,[9] delocalized charge transport,[16] multiple trapping and release,[17,18] and other hybrid models.[19] Most of these studies have been conducted on a variety of organic semiconductors grown on different dielectric insulators (where the dielectric constant spans from low κ to high κ values). A recent work by Senanayak *et al.* shows that copolymers of PVDF permit an order of magnitude change in the polarization with temperature.[20] In particular, κ changes from 4 to 24 in PVDF-TrFE when the temperature is varied from 200 K to the ferroelectric-paraelectric phase transition at 390 K (T_c). By using the same organic semiconductor-insulator interface, PVDF-TrFE allows a platform for understanding transport as the polarization strength is tuned from a weak-to strong-coupling regime with changing temperature (T).

The ferroelectric properties of PVDF arise from the differing electronegativity of hydrogen and fluorine, which gives rise to a dipole for each molecule oriented perpendicular to the polymer chain (as shown in Fig. 1). The ferroelectric phase occurs in the all-trans or β-phase of the polymer. The copolymer, PVDF-TrFE, has the advantage of being ferroelectric directly after solution processing of the film, while PVDF requires additional measures such as stretching or controlled heating of the film to ensure all trans-configuration.[21,22] It has been shown that solvents used for dissolving PVDF-TrFE impact device performance. High dipole moment solvents, such as dimethyl sulfoxide (DMSO), enhance the remnant polarization in PVDF-TrFE-based capacitors.[23] Compared to other solvents, DMSO dissolved PVDF-TrFE capacitors show a hysteresis in the displacement curve even at very low

[a)]Electronic mail: guhas@missouri.edu

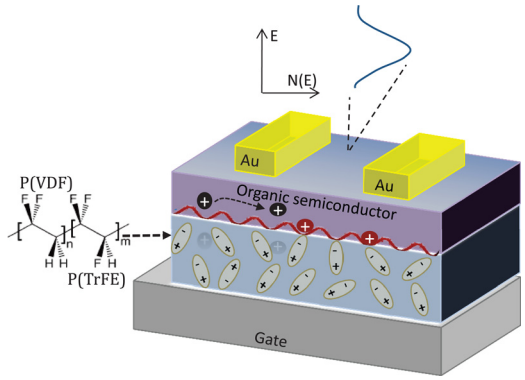

FIG. 1. Schematic of a ferroelectric-based OFET where the dynamic coupling of charge carriers to the electronic polarization at the semiconductor-dielectric is illustrated. In addition to the bulk disorder within the semiconductor, there is trapping of charges at the interface.

voltages, indicating that the dipoles in the copolymer are ordered initially. As seen in Ref. 20, the ferroelectric environment in PVDF-based copolymers has a strong contribution to polarization fluctuation driven transport (which is reflected in the strong T-dependence of κ) compared to the static dipolar induced disorder observed in non-polar dielectrics.

This investigation is motivated by the work of Senanayak *et al*. where temperature-dependent transport characteristics of P3HT (polythiophene) OFETs with PVDF and its copolymers as the dielectric layer were determined.[20] In this work, we employ pentacene as the organic semiconductor, mainly, so that we can compare our experimental results with theory as well as compare the temperature dependent transport characteristics of pentacene OFETs with other non-polar dielectrics, as discussed in Sec. III A. In Sec. III B, we compare the temperature-dependent charge carrier mobility of pentacene OFETs with varying thicknesses of the PVDF-TrFE layer from 20 nm to 500 nm. For all cases, a thermally activated hopping mechanism is observed, where the activation energy decreases beyond the ferroelectric to paraelectric phase transition temperature of PVDF-TrFE. The trapped charge density shows a slight increase till T_c, beyond which it decreases in the paraelectric phase. By comparing single layer PVDF-TrFE OFETs to stacked PVDF-TrFE/SiO_2 devices, the polarization fluctuation dependent mobility, μ_p, is decoupled from the regular temperature-dependent mobility in Sec. III C. By fits to a small polaron model, the hopping distance is estimated and is found to be the largest for the 500 nm thick OFET, consistent with the slightly larger charge carrier mobility of the thicker dielectric devices compared to the thinner dielectric devices.

II. EXPERIMENTAL DETAILS

A. Materials

Pentacene was procured from Tokyo Chemical Industry and used as is without any purification. Dielectric materials poly[(vinylidenefluoride-co-trifluoroethylene] (PVDF-TrFE) (75/25)and Poly(methyl methacrylate) (PMMA, Mw 996 000) were obtained from Measurement Specialties, Inc., USA and Sigma Aldrich, Inc., respectively. The solvents N,N-Dimethylformamide (DMF) and DMSO were procured from Sigma Aldrich, Inc. The glass substrates and SiO_2 on Si^{++} wafers were obtained from Fisher Scientific and Silicon Quest International, respectively.

B. Device preparation and characterization

Bottom gate, top contact single dielectric layer OFETs were fabricated by evaporating 60 nm aluminum as gate electrode on organically cleaned glass substrates using a shadow mask. The dielectric layers were obtained by spin coating the polymer dielectric solution. 1.8 wt. %, 2 wt. %, 3.5 wt. %, 4 wt. %, 4.5 wt. %, and 16 wt. % of PVDF-TrFE in DMF solution were heated at 80 °C to completely dissolve the solute. A few drops of the solution were dropped onto Al coated glass slides and spin coated at 1600 rpm for 60 s. The films were vacuum annealed at 135 °C for an hour and a half to improve the crystallinity. The different concentrations resulted in the thickness of the dielectric film to vary from 20 nm to 500 nm. The thicknesses of the films were measured by a reflectometer (Mprobe, Inc.) and further confirmed by a profilometer and an atomic force microscope (AFM). 6 wt. % of PMMA in DMSO solution was magnetically stirred and heated at 75 °C for 45 min and then spin coated on Al coated glass slides at 5000 rpm for 60 s. The resulting thickness of the PMMA film was 150 nm. The PMMA film was further baked at 100 °C for 20 min. All dielectric films were followed by a 60 nm film of thermally evaporated pentacene (10^{-5} mbar, 0.3 Å/s). Finally, 50 nm Au source drain top contacts (10^{-5} mbar, 3.0 Å/s) were thermally deposited. The channel width (W) to length (L) ratio was 40 for most of the devices, with $W = 2000\ \mu$m and L = 50 μm.

Stacked bilayer OFETs were fabricated by spin coating PVDF-TrFE (using the same recipe as for the single layer) on SiO_2/Si^{++} wafers. Prior to depositing the polymer dielectric layer, the SiO_2 wafers organically cleaned. This was then followed by pentacene and Au deposition.

Room temperature DC electrical characterizations were performed using two source meters, Keithley 2400 and Keithley 236, using a customized LabVIEW program. For temperature-dependent electrical measurements, a dual source meter Keithley 2612B was used. The OFETs were kept inside a closed-cycle helium cryostat (APD Cryogenics) where the temperature may be varied from 11 K to 480 K. The temperature was measured using a Lakeshore 330 temperature controller. All PVDF-TrFE-based devices were measured from 200 K to 450 K. To test for reversibility, some devices were also measured from high temperature to low temperature. The capacitance measurements from metal-insulator-metal and metal-insulator-semiconductor diodes were carried out with an HP 4284A precision LCR meter.

The electrical parameters of the OFETs were obtained from the saturation region of the transconductance curves by using $\mu = \frac{2L}{WC_i}\left(\frac{\partial\sqrt{I_{ds}}}{\partial V_g}\right)^2$, where C_i is the dielectric capacitance, W is the channel width, L is the channel length, V_g is the gate voltage, I_{ds} is the drain current, and μ is the field-effect mobility.

The Raman spectra were collected by an Invia Renishaw spectrometer attached to a confocal microscope with 50× long objective lens using an excitation wavelength of 785 nm from a diode laser. The samples were affixed to a

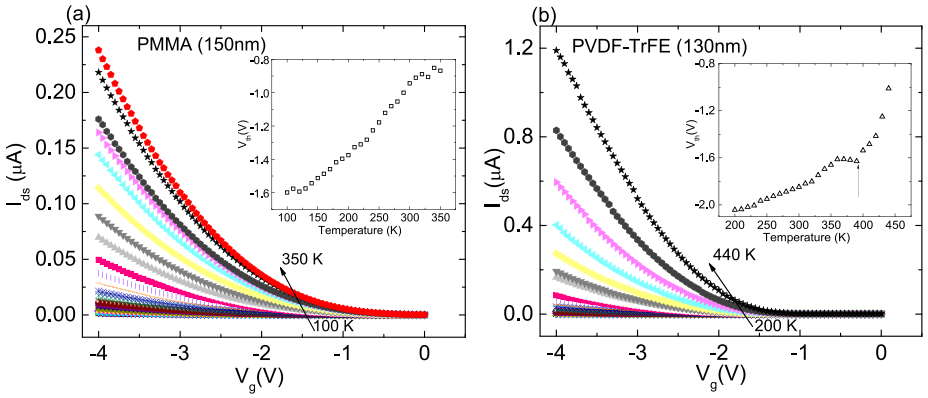

FIG. 2. (a) Transfer curves at different temperatures from 100 K to 350 K for a pentacene OFET with PMMA as the dielectric layer. (b) Transfer curves at different temperatures from 200 K to 440 K for a pentacene OFET with PVDF-TrFE as the dielectric layer. In both cases, $V_{ds} = -4$ V. The insets show the threshold voltage as a function of temperature.

stainless steel sample holder of a Linkam LTS350 microscope hot-cold stage.

III. RESULTS AND DISCUSSIONS

A. Comparison of polar versus non-polar dielectric

Thermally activated transport in pentacene OFETs (using non-ferroelectric dielectrics) has been observed by many groups.[24–26] Other acene-based semiconductors also show activated transport with a distinct relationship between the contact-induced film microstructure and charge carrier mobility.[27] Since pentacene has many grain boundaries, rather than a bandlike transport, a thermally activated hopping of charges from site to site within a disorder induced exponential distribution of states, as proposed by Monroe,[28] is observed. In such a mechanism, the charge carrier mobility, μ, is given by

$$\mu = \mu_0 \exp\left(-\frac{\Delta}{k_B T}\right), \tag{1}$$

where Δ, the activation energy, is the energetic difference between the Fermi energy and the transport level, μ_0 is the mobility in the absence of any trap states, and k_B is the Boltzmann constant. Additionally, as the charge carrier density increases, the Fermi energy gets closer to the transport level, easing the transport of charges and thus decreasing Δ. Within the context of transport in OFETs, the above model is more complex, especially when the polarization field of the dielectric interface needs to be considered. By comparing PVDF-TrFE-based OFET characteristics to non-polar dielectric OFETs, the effect of the polarization field can be readily observed.

Fig. 2 shows the transconductance curves of PMMA and PVDF-TrFE OFETs at various temperatures. The insets show the threshold voltage as a function of temperature. As expected in an activated transport mechanism, the threshold voltage decreases with increasing temperature in both cases; however, the PVDF-TrFE sample shows a discontinuity at the ferroelectric-paraelectric phase transition temperature, beyond which the rate of increase in V_{th} is much higher compared to in the ferroelectric phase. As we see later, a higher V_{th} can be accounted for by a decrease in the trapped charge density. For the transfer characteristics at each temperature, the gate voltage was swept up to V_{ds}, which was in the saturation region.

Fig. 3 shows the charge carrier mobility of pentacene OFETs as a function of temperature with PMMA (150 nm thickness) and PVDF-TrFE (130 nm thickness) as dielectric layers. All mobilities are extracted in the saturation region as explained in Sec. II B. We point out that both PMMA and PVDF-TrFE devices operate below −4 V. At room temperature, the charge carrier mobility of the PMMA-based OFET in the saturation region (0.03 cm^2/V s) is an order of magnitude lower compared to our prior work (where PMMA was dissolved in a high dipole moment solvent),[29] primarily due to the higher thickness of the dielectric layer in this work. Since PMMA degrades at higher temperatures, the pentacene/PMMA OFET measurements were carried out only till 350 K. The PVDF-TrFE-based OFETs were tracked all the way from the ferroelectric phase to above T_c. Agreeably, the charge carrier density may differ at the two dielectric interfaces but there are clear differences in the nature of the transport in the two devices. The PMMA device shows a sharp increase in its mobility with increasing temperature, whereas the PVDF-TrFE device shows a suppressed mobility in the ferroelectric phase, beyond which there is a large change in its mobility. The dielectric constant of PVDF-TrFE as a function of temperature is also plotted.[20] The discontinuity at 390 K denotes the ferroelectric to the paraelectric phase.

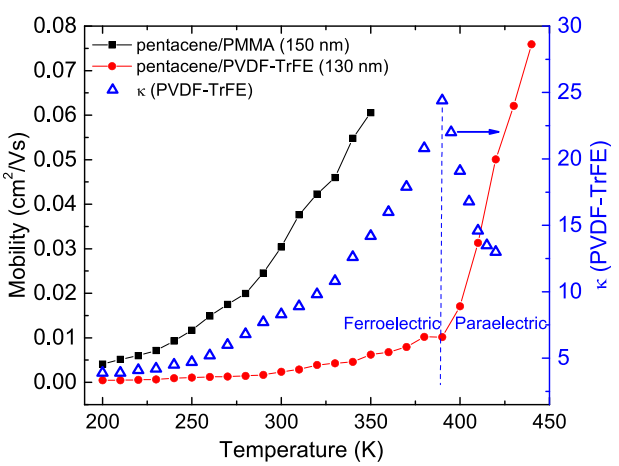

FIG. 3. Comparison of the charge carrier mobility as a function of temperature in pentacene OFETs using PMMA and PVDF-TrFE as dielectric layers. The dielectric constant of PVDF-TrFE as a function of temperature shown in the figure is from Ref. 20.

The suppression of the charge carrier mobility with increasing temperature in the ferroelectric phase may be attributed to a coupling of the charge carriers to the dielectric polarization of the gate insulator, resulting in a renormalization of the transfer integral, J. The dynamic coupling thus reduces J to J^*, thereby increasing the effective mass (m^*) of the carriers. Theoretical calculations show that m^* increases by a factor of 1.27 in bulk pentacene due to molecular polarization effects.[13] In order to understand whether there is a universality of the dynamical coupling due to the polarization effect and to distinguish between surface and bulk effects, we have carried out detailed temperature-dependent current-voltage (I-V) measurements from pentacene OFETs by varying the thickness of the PVDF-TrFE layer. These results are presented in the next section.

B. Thickness-dependence of the ferroelectric layer

The thickness of the PVDF-TrFE layer was varied from 20 nm to 500 nm; the pentacene layer thickness was kept the same at 60 nm for all OFETs. All devices show a similar trend for charge carrier mobilities versus temperature as shown in Fig. 3, where μ_{FET} shows a sharp increase beyond the ferroelectric-paraelectric phase transition at 390 K. Fig. 4 shows the Arrhenius plots for OFET mobilities in the ferroelectric phase for varying thicknesses of the PVDF-TrFE layer. The 20 nm device (not shown here) shows an activation energy of 88 meV. We note that the activation energies (Δ) obtained by fits to Eq. (1) are much higher here than typically seen for pentacene OFETs with non-ferroelectric dielectrics.[26] Furthermore, the correction due to thermalization of individual dipoles (as a result of the nonlinear contribution) when the system approaches T_c has not been taken into account here.[20] Taking this correction may slightly reduce the mobility in the ferroelectric phase, thus further enhancing Δ. Since the OFETs in this work are low operating voltage devices, the nonlinear contribution may not be that high as evident from a prior work on polarization measurements from PVDF-TrFE capacitors with similar thicknesses.[23]

The trend in Fig. 4 clearly shows the activation energy to decrease with increasing thickness of the dielectric layer. This observation is consistent with slightly higher values of μ_{FET} for thicker layers of PVDF-TrFE. In the ferroelectric region, there are thus two competing effects: activated hopping transport, which tends to increase μ_{FET} with increasing temperatures, and the coupling of the carriers to the electric polarization in the form of surface Fröhlich polarons as κ increases with temperature, which tends to decrease μ_{FET}. The thinner dielectric layers induce stronger polarization fields, suppressing the charge carrier mobility even more compared to the thicker dielectric layers in the ferroelectric region.

The trapped charge density (N_{trap}^{max}), which is obtained from the subthreshold swing, as a function of temperature offers insights into the mechanism of transport in ferroelectric OFETs. It is given by

$$N_{trap}^{max} \approx \left[\frac{qS\log(e)}{k_BT} - 1\right]\frac{C_i}{q}, \tag{2}$$

where q is the elementary charge and C_i is the gate capacitance per unit area. The subthreshold swing, S, is given by $S = [\frac{d\log(I_{ds})}{dV_g}]^{-1}$. Equation (2) typically yields the maximum trapped charge. Using the change in V_{th} from I-V hysteresis measurements yields a lower limit of the trapped charge density.[30] At room temperature, S varies from 0.3 V/dec to 2 V/dec for the different thicknesses of the PVDF-TrFE layer. Fig. 5 plots N_{trap}^{max} for three PVDF-TrFE devices as a function of temperature. Beyond T_c, there is a sharp decrease in the trapped charge density, which explains the large enhancement of μ_{FET} in the paraelectric phase. The overall value of the trapped charge density decreases almost monotonically from 20 nm to 130 nm, indicating that the surface states dominate in the thinner films. The inset in Fig. 5 compares the trapped charge density of the PMMA device with a similar thickness PVDF-TrFE device. Although the PMMA-based device has a higher value of N_{trap}^{max} between 200 K and 300 K, it shows a much higher value of μ_{FET} compared to the PVDF-TrFE device in this temperature regime (Fig. 3). These observations clearly show that the lower and the almost temperature-independent mobility in the ferroelectric

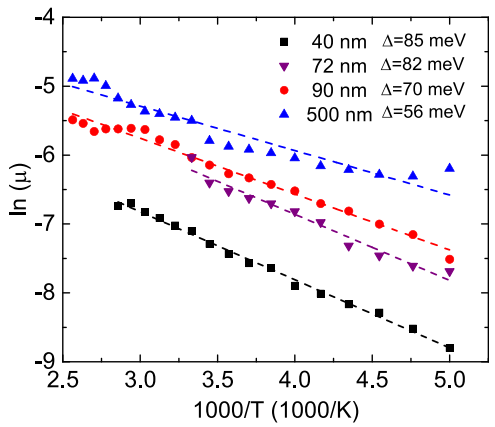

FIG. 4. Arrhenius plots of OFET mobilities in the ferroelectric phase for varying thicknesses of the PVDF-TrFE layer.

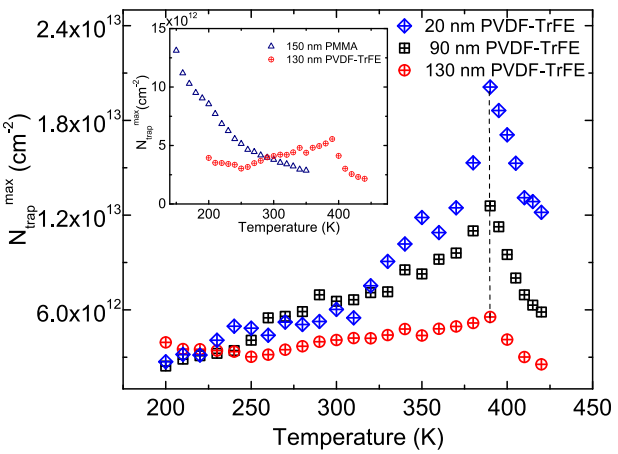

FIG. 5. The trapped charge density as a function of temperature for the 20 nm, 90 nm, and 130 nm thick PVDF-TrFE devices. The inset compares the trapped charge density of the PMMA-based pentacene OFET with a PVDF-TrFE-based OFET.

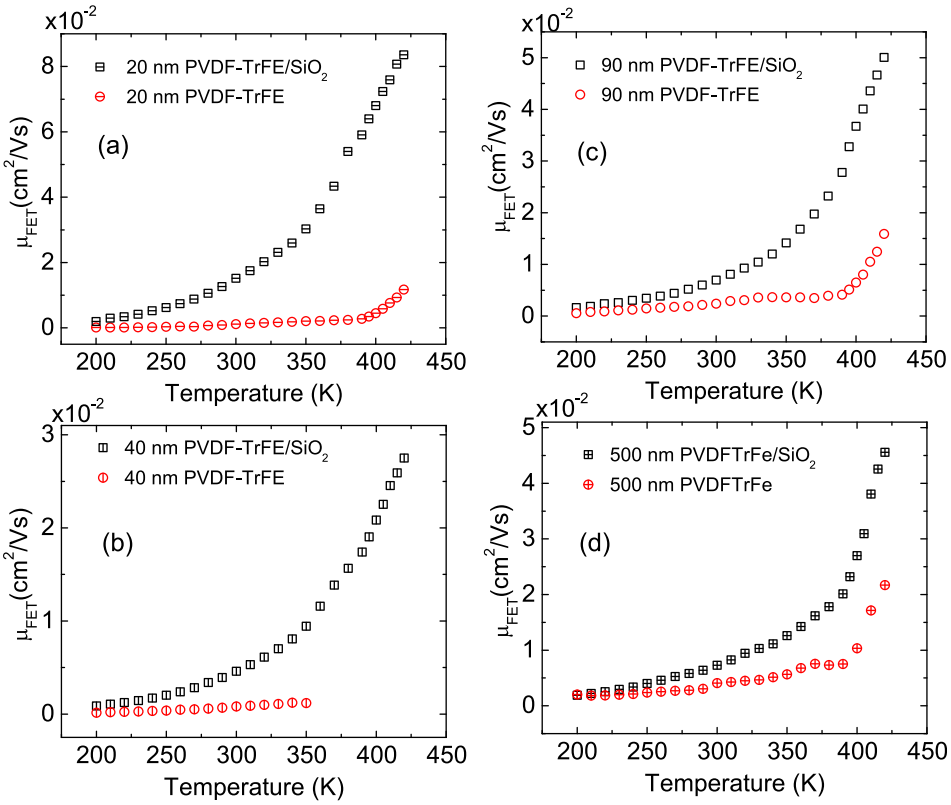

FIG. 6. Comparison of single layer PVDF-TrFE and stacked PVDF-TrFE/SiO_2 OFETs with (a) 20 nm, (b) 40 nm, (c) 90 nm, and (d) 500 nm of the PVDF-TrFE thickness.

phase of PVDF-TrFE OFETs originate from a polarization fluctuation driven transport that dominates over the energetic disorder processes (observed in non-polar dielectrics).

C. Stacked PVDF-TrFE/inorganic layers

In order to distinguish the thermal process from the polarization contribution to the mobility (μ_{FET}), stacked OFETs were prepared where the PVDF-TrFE film was grown on 200 nm of SiO_2. The μ_{FET} mobilities for four such pairs of devices are shown in Fig. 6, where the PVDF-TrFE film was identical for the single and stacked layers. In the stacked devices, the organic semiconductor-ferroelectric interface is still maintained, but since the gate electrode is now in contact with a non-ferroelectric dielectric, no effective change in polarization is expected. The stacked device is thus dominated by a "typical" temperature-dependent hopping transport, whereas the single ferroelectric-based OFET is dominated by polarization fluctuations in the ferroelectric phase (below T_c). Assuming that the ferroelectric component of the stacked device contributes negligibly to transport, the mobility ($\mu_{stacked}$) as a function of temperature may be used as a reference to take into account the contribution from all additional factors. By using the Matthiessen's rule, $\mu_{FET} = (1/\mu_P + 1/\mu_{stacked})^{-1}$, the contribution due to the Fröhlich polarons (polarization fluctuation dependent mobility), μ_P, may be extracted from the knowledge of the temperature dependence of the mobility of single layer ferroelectric and stacked devices.

The strongly coupled Fröhlich polaron model[31] yields

$$\mu_P(T) = \frac{ea^2\omega_s}{8k_BT}\exp\left(-\frac{\Delta_P}{k_BT}\right), \quad (3)$$

where ω_s is the frequency of the surface phonons of the dielectric, a is the hopping length, and Δ_P is the polaron hopping barrier. We note that ω_s is related to the longitudinal (ω_L) and transverse (ω_T) optical phonon frequencies by $\omega_s^2 = \frac{1}{2}(\omega_L^2 + \omega_T^2)$. The factor of 8 in the denominator results from considering an upper bound to the mobility in the hopping process. The Einstein's relation for a nondegenerate carrier gas yields $\mu = \frac{qD}{k_BT}$, where D, the diffusion coefficient, is given by $\gamma a^2/4$ in two dimensional hopping motion, and γ is the hopping rate. The probability of hopping takes on a factor of 1/2 for each attempt to pass the barrier in the forward direction.[13]

Fig. 7 shows the temperature-dependent mobility of Fröhlich polarons for OFETs with 500 nm, 90 nm, and 40 nm

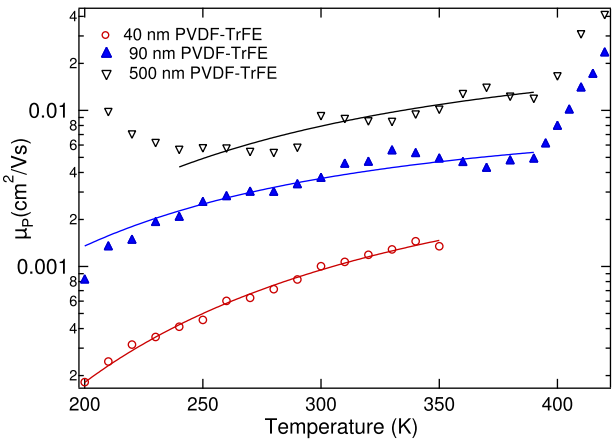

FIG. 7. Temperature-dependent mobility of Fröhlich polarons for pentacene OFETs with three thicknesses of the PVDF-TrFE layer. The bold line is a fit to the model discussed in the text.

TABLE I. The polaron hopping barrier and hopping lengths obtained by fits to Eq. (3).

Thickness of PVDF-TrFE (nm)	Δ_P (eV)	a (Å)
500	0.085 ± 0.007	5.55 ± 0.70
90	0.078 ± 0.005	2.90 ± 0.30
40	0.107 ± 0.004	2.85 ± 0.20
20	0.096 ± 0.009	2.37 ± 0.40

thick PVDF-TrFE layers, which were extracted by comparing the single layer devices with the stacked layers as explained above. The experimental data in the ferroelectric phase were fit with Eq. (3), and the parameters are tabulated in Table I. For clarity, we do not include the 20 nm data in Fig. 7. We use $\omega_s = 500\,\text{cm}^{-1}$ in the fits, which is reasonable since the β phase of PVDF is characterized by ω_L and ω_T at $\approx 500\,\text{cm}^{-1}$.[32,33] The hopping length increases with the thickness of the PVDF-TrFE layer, consistent with the slightly larger mobilities observed for the thicker dielectric devices. For single crystals such as rubrene, which show at least two orders of magnitude higher FET mobility compared to this work, the hopping length is theoretically found to be greater than 7 Å.[13]

One can further estimate the polaron binding energy from the polaron hopping barrier. The hopping barrier is related to the binding energy, E_P, by $\Delta_P \approx \frac{1}{2}E_P - J^*$. Using the value of $J^* = 44.9\,\text{meV}$ for a pentacene/Ta_2O_5 interface from Ref. 13, $E_P \approx 260\,\text{meV}$ for the 500 nm device, suggesting that the strongly coupled polaron model is appropriate to describe transport for polycrystalline pentacene OFETs with a ferroelectric dielectric. Such a moderately high binding energy also explains the low and almost temperature-independent μ_{FET} in the ferroelectric phase. For a rubrene/Ta_2O_5 interface, the polaron binding energy was theoretically obtained as $\approx 100\,\text{meV}$.[13]

D. Raman scattering from pentacene on PVDF-TrFE

One of the questions that arise is whether the change in the transport properties of pentacene OFETs on PVDF-TrFE is related to an electron-phonon coupling mechanism originating from the semiconductor layer itself. Reports on the phase transition of PVDF and its copolymers have been followed by Raman scattering.[34] Fig. 8 shows the Raman spectra of pentacene from 1100 to 1700 cm^{-1} from room temperature to above T_c of the dielectric layer. The aromatic stretch vibration lies in the 1340–1400 cm^{-1} range. The two peaks at 1160 and 1178 cm^{-1} are related to C-H bending motion. The 1371 cm^{-1} peak is seen as the strongest C-C stretch vibration. Details of the Raman spectrum of pentacene are found in Ref. 35. As such, there are no abrupt changes in the Raman phonon frequencies or line shapes of pentacene as the underlying PVDF-TrFE layer undergoes a phase transition. A softening of the Raman frequencies with increasing temperature is observed, which is typical for any solid. Furthermore, we have also compared the Raman spectrum of pentacene on a non-polar dielectric layer with similar temperature sweeps as on PVDF-TrFE; the slight changes in the frequencies and broadening of the Raman peaks with temperature are identical on both interfaces. These results conclusively show that changes in the transport properties arise from a coupling of the carriers with the dielectric interface.

IV. CONCLUSIONS

The charge transport in ferroelectric-based OFETs is strongly influenced by a polarization dominant transport rather than an energetic disorder within the framework of a hopping transport. The ferroelectric dielectric, PVDF-TrFE, which shows a large change in its dielectric constant as the temperature is swept from 200 K to the ferroelectric-paraelectric phase transition temperature at 390 K, provides a testbed to study interfacial transport as the polarization strength is tuned. When the gate insulator is sufficiently polar, Fröhlich polarons play an important role in interfacial transport. Temperature-dependent charge carrier mobility in pentacene OFETs shows almost no change as long as the

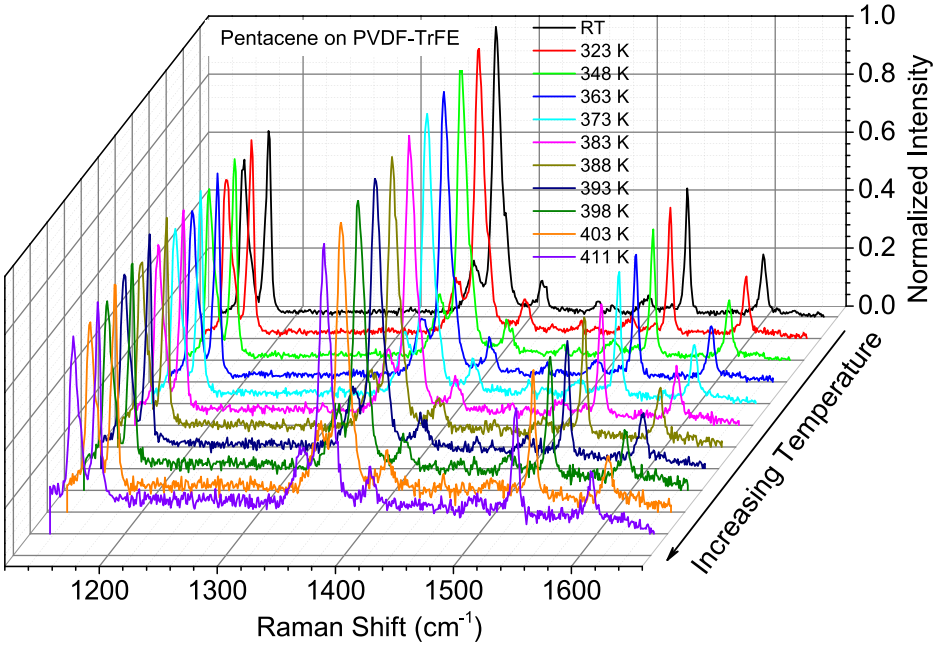

FIG. 8. Raman spectra of pentacene on PVDF-TrFE as a function of temperature.

dielectric layer is in the ferroelectric phase due to the coupling of the charge carriers with the surface phonons of the dielectric layer. This effect is more pronounced for thinner dielectric films. The threshold voltage and the trapped charge density also show a discontinuity at the ferroelectric-paraelectric phase transition.

To extract the polarization contribution to the temperature dependence of the charge carrier mobility from mechanisms other than Fröhlich polarons, ideally one should look at a pentacene OFET where the gate insulator is vacuum. This is clearly not an option for a polycrystalline film such as pentacene. By fabricating stacked PVDF-TrFE/SiO_2 dielectrics, the surface between pentacene and PVDF-TrFE remains unchanged but since the gate electrode is in contact with the SiO_2 layer, the polarization field is absent. The stacked devices show a typical temperature-dependent mobility as seen with non-polar dielectrics. By comparing the stacked devices with single layer PVDF-TrFE pentacene OFETs, temperature-dependent mobility (due to the polarization fluctuation) was extracted. Using a strongly coupled Fröhlich polaron model, we estimate the hopping length and the hopping barrier of the polarons. The hopping lengths vary between 2 Å and 5 Å. Ferroelectric dielectrics, where the polarization strength can be tuned with temperature, thus provide a mechanism for understanding transport in the rapidly growing field of small molecule and polymer-based thin film transistors.

ACKNOWLEDGMENTS

We acknowledge the support of this work through the National Science Foundation under Grant No. ECCS-1305642.

[1]H. Kawai, Jpn. J. Appl. Phys., Part 1 **8**, 975 (1969).
[2]A. J. Lovinger, Science **220**, 1115 (1983).
[3]S. Fujisaki, H. Ishiwara, and Y. Fujisaki, Appl. Phys. Lett. **90**, 162902 (2007).
[4]R. C. G. Naber, P. W. M. Blom, A. W. Marsman, and D. M. de Leeuw, Appl. Phys. Lett. **85**, 2032 (2004).
[5]R. C. G. Naber, C. Tanase, P. W. M. Blom, G. H. Gelink, A. W. Marsman, F. J. Touwslager, S. Setayesh, and D. M. De Leeuw, Nat. Mater. **4**, 243 (2005).
[6]C. A. Nguyen, S. G. Mhaisalkar, J. Ma, and P. S. Lee, Org. Electron. **9**, 1087 (2008).
[7]Y. Zheng, G.-X. Ni, C.-T. Toh, C.-Y. Tan, K. Yao, and B. Özyilmaz, Phys. Rev. Lett. **105**, 166602 (2010).
[8]E. Conwell, in *Primary Photoexcitations in Conjugated Polymers: Molecular Exciton Versus Semiconductor Model*, edited by N. S. Sariciftci (World Scientific, 1997).
[9]M. C. J. M. Vissenberg and M. Matters, Phys. Rev. B **57**, 12964 (1998).
[10]H. Bässler, Phys. Status Solidi B **175**, 15 (1993).
[11]V. Coropceanu, J. Cornil, D. A. da Silva Filho, Y. Olivier, R. Silbey, and J.-L. Bredas, Chem. Rev. **107**, 926 (2007).
[12]H. Houili, J. D. Picon, L. Zuppiroli, and M. N. Bussac, J. Appl. Phys. **100**, 023702 (2006).
[13]S. J. Konezny, M. N. Bussac, and L. Zuppiroli, Phys. Rev. B **81**, 045313 (2010).
[14]I. N. Hulea, S. Fratini, H. Xie, C. L. Mulder, N. N. Iossad, G. Rastelli, S. Ciuchi, and A. F. Morpurgo, Nat. Mater. **5**, 982 (2006).
[15]Y. Xia, J. H. Cho, J. Lee, P. P. Ruden, and C. D. Frisbie, Adv. Mater. **21**, 2174 (2009).
[16]S. E. Koh, B. Delley, J. E. Medvedeva, A. Facchetti, A. J. Freeman, T. J. Marks, and M. A. Ratner, J. Phys. Chem. B **110**, 24361 (2006).
[17]R. J. Chesterfield, J. C. McKeen, C. R. Newman, C. D. Frisbie, P. C. Ewbank, K. R. Mann, and L. L. Miller, J. Appl. Phys. **95**, 6396 (2004).
[18]R. J. Chesterfield, J. C. McKeen, C. R. Newman, P. C. Ewbank, D. A. da Silva, J. L. Bredas, L. L. Miller, K. R. Mann, and C. D. Frisbie, J. Phys. Chem. B **108**, 19281 (2004).
[19]K. Waragai, H. Akimichi, S. Hotta, H. Kano, and H. Sakaki, Phys. Rev. B **52**, 1786 (1995).
[20]S. P. Senanayak, S. Guha, and K. S. Narayan, Phys. Rev. B **85**, 115311 (2012).
[21]M. Li, H. J. Wondergem, M.-J. Spijkman, K. Asadi, I. Katsouras, P. W. M. Blom, and D. M. deLeeuw, Nat. Mater. **12**, 433 (2013).
[22]T. Furukawa, IEEE Trans. Electron. Insul. **24**, 375 (1989).
[23]G. Knotts, A. Bhaumik, K. Ghosh, and S. Guha, Appl. Phys. Lett. **104**, 233301 (2014).
[24]D. Knipp, R. A. Street, A. Vlkel, and J. Ho, J. Appl. Phys. **93**, 347 (2003).
[25]D. Guo, T. Miyadera, S. Ikeda, T. Shimada, and K. Saiki, J. Appl. Phys. **102**, 023706 (2007).
[26]L. Dunn and A. Dodabalapur, J. Appl. Phys. **107**, 113714 (2010).
[27]D. J. Gundlach, J. E. Royer, S. K. Park, S. Subramanian, O. D. Jurchescu, B. H. Hamadani, A. J. Moad, R. J. Kline, L. C. Teague, O. Kirillov, C. A. Richter, J. G. Kushmerick, L. J. Richter, S. R. Parkin, T. N. Jackson, and J. E. Anthony, Nat. Mater. **7**, 216 (2008).
[28]D. Monroe, Phys. Rev. Lett. **54**, 146 (1985).
[29]N. B. Ukah, J. Granstrom, R. R. S. Gari, G. M. King, and S. Guha, Appl. Phys. Lett. **99**, 243302 (2011).
[30]W. Xu and S.-W. Rhee, J. Mater. Chem. **19**, 5250 (2009).
[31]I. G. Austin and N. F. Mott, Adv. Phys. **18**, 41 (1969).
[32]K. Tashiro, Y. Itoh, M. Kobayashi, and H. Tadokoro, Macromolecules **18**, 2600 (1985).
[33]S. M. Nakhmanson, R. Korlacki, J. T. Johnston, S. Ducharme, Z. Ge, and J. M. Takacs, Phys. Rev. B **81**, 174120 (2010).
[34]K. Tashiro and M. Kobayashi, Polymer **29**, 426 (1988).
[35]D. Adil and S. Guha, J. Chem. Phys. **139**, 044715 (2013).